Applying this to the Hermitian matrix A,

$$\partial \det A/\partial \alpha_{kl} = ia_{kl} b_{lk} \det A - ia_{lk} b_{kl} \det A, \quad (A6)$$

which after some simplification becomes

$$\partial \det A/\partial \alpha_{kl} = 2|a_{kl}||b_{kl}| \sin(\beta_{kl} - \alpha_{kl}) \det A. \quad (A7)$$

References

BAGGIO, R. & WOOLFSON, M. M. (1978). *Acta Cryst.* A**34**, 883–892.

FREER, A. A. & GILMORE, C. J. (1980). *Acta Cryst.* A**36**, 470–475.

GILMORE, C. J. (1977). *Acta Cryst.* A**33**, 712–716.

GOEDKOOP, J. A. (1952). *Computing Methods and the Phase Problem in X-ray Crystal Analysis*, edited by R. PEPINSKY, pp. 61–83. The Pennsylvania State College.

HEINERMANN, J. J. L., KROON, J. & KRABBENDAM, H. (1979). *Acta Cryst.* A**35**, 101–105.

HOOGENDORP, J. & ROMERS, C. (1982). *Acta Cryst. B*. In the press.

KARLE, J. & HAUPTMAN, H. (1950). *Acta Cryst.* **3**, 181–187.

KITAIGORODSKY, A. I. (1950). *X-ray Structure Analysis*, Vol. III, p. 61. Moscow: Gostekhizdat.

KNOSSOW, M., RANGO, C. DE, MAUGUEN, Y., SARRAZIN, M. & TSOUCARIS, G. (1977). *Acta Cryst.* A**33**, 119–125.

KOENERS, H. J., KOK, A. J. DE, ROMERS, C. & BOOM, J. H. VAN (1980). *Recl Trav. Chim. Pays-Bas*, pp. 355–362.

KOK, A. J. DE, BOOMSMA, F. & ROMERS, C. (1976). *Acta Cryst.* B**32**, 2492–2496.

KOK, A. J. DE & ROMERS, C. (1975). *Acta Cryst.* B**31**, 1535–1542.

KOK, A. J. DE, ROMERS, C. & HOOGENDORP, J. (1975). *Acta Cryst.* B**31**, 2818–2823.

MAIN, P. (1975). *Crystallographic Computing Techniques*, edited by F. R. AHMED, pp. 165–175. Copenhagen: Munksgaard.

NAG: NUMERICAL ALGORITHMS GROUP (1978). *NAG Fortran Library Manual*, Mark 7. Oxford Univ. Press.

NAVAZA, J. & SILVA, A. M. (1979). *Acta Cryst.* A**35**, 266–275.

RANGO, C. DE, MAUGEN, Y. & TSOUCARIS, G. (1975). *Acta Cryst.* A**31**, 227–233.

RANGO, C. DE, MAUGUEN, Y., TSOUCARIS, G., DODSON, G. G., DODSON, E. J. & TAYLOR, D. J. (1979). *J. Chim. Phys. Phys. Chim. Biol.* **76**, 811–812.

TAYLOR, D. J., WOOLFSON, M. M. & MAIN, P. (1978). *Acta Cryst.* A**34**, 870–883.

TSOUCARIS, G. (1970). *Acta Cryst.* A**26**, 492–494.

VERMIN, W. J. & GRAAFF, R. A. G. DE (1978). *Acta Cryst.* A**34**, 892–894.

Acta Cryst. (1982). A**38**, 470–476

Crystalline Modifications and Structural Phase Transitions of NaOH and NaOD

BY H.-J. BLEIF AND H. DACHS

Hahn-Meitner-Institut für Kernforschung, Glienicker Strasse 100, *D*-1000 *Berlin* 39, *Federal Republic of Germany*

(*Received* 10 *February* 1981; *accepted* 4 *February* 1982)

Abstract

Structural work on the three modifications of sodium hydroxide is reviewed. The monoclinic and cubic modifications were determined with neutron and X-ray diffraction, respectively. The phase-transition temperatures were determined by specific-heat measurements. The cubic to monoclinic transition is a first-order transition with a freezing of the rotational motion of the OH (and OD) groups. The monoclinic axes **a**, **b** and **c*** tend to be oriented parallel to the original cubic directions $[\bar{1}\bar{1}2]$, $[1\bar{1}0]$ and [111], respectively. The orthorhombic to monoclinic transition is a nearly continuous displacive phase transition with a soft acoustic shear mode. The order parameter is the homogeneous shear of the crystal in the **a** direction. Its temperature dependence is described within Landau theory.

1. Introduction

The low-temperature orthorhombic modification of NaOH was determined by Ernst (1946) with some speculations on the position of the hydrogen atom. Stehr (1967) determined the H positions with neutron scattering and found a monoclinic modification $P2_1/m$ at higher temperatures. Bleif (1971) found from specific-heat measurements and X-ray diffraction patterns that there are three different modifications as a function of temperature, the high-temperature phase being cubic $Fm3m$, as suggested by West (1935). The

0567-7394/82/040470-07$01.00

three different structures of NaOH (and NaOD) are shown in Fig. 1 and the corresponding parameters are summarized in Table 1. The face-centered monoclinic unit cell depicted in Fig. 1 shows the close relationship between the orthorhombic and monoclinic structures. For display purposes, the origin was chosen at the oxygen site. In Fig. 4 and Table 1 the origin is at a center of inversion. Starting from the cubic modification, the monoclinic and orthorhombic structures could be reached by displacing (001) double layers in the [110] direction. In fact, the cubic to monoclinic transition proceeds somewhat differently (see § 6). In the orthorhombic and approximately also in the monoclinic phase, Na, O and H form linear groups perpendicular to the (001) plane. The layers still have the NaCl structure with respect to Na and O, and they are stacked along **c*** with an interval of about 5·7 Å.

The transition between the monoclinic and the cubic modification is discontinuous. The heat involved in the transformation is 6·36 kJ mol^{-1} (Douglas & Dever, 1954) and is equal to the melting enthalpy. The OH groups must be orientationally disordered in the cubic phase to fit into the cubic symmetry, and the great heat of transformation is characteristic of the onset of rotational motion. The orthorhombic to monoclinic transition is due to an almost continuous displacement of successive layers in the **a** direction, which increases with temperature up to a value of 0·14 times the lattice constant (corresponding to a shear angle of 5°). It is shown in § 7 that the phase transition can be described within Landau theory. There are differences in the temperature dependence of the order parameter between single crystals and powder specimens. This can be accounted for by introducing an external field H into the Landau free-energy expansion, which couples to the order parameter.

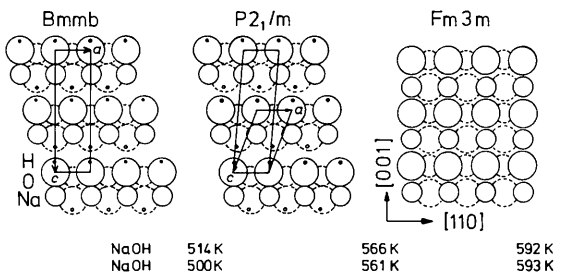

Fig. 1. Crystalline modifications and transition temperatures of NaOH and NaOD. The O–H distance is about 0·9 Å, so that the proton is within the ionic radius of O^{2-}. Solid and dashed lines represent atoms at $y = \frac{1}{4}$ and $-\frac{1}{4}$, respectively. The choice of the origin for the orthorhombic and monoclinic structures is non-standard and is different from the choice adopted in Fig. 4 and Table 1.

Table 1. *Structural data for three crystalline modifications of* NaOH

The temperature factor is

$$T = \exp[-2\pi^2 (U_{11}h^2a^{*2} + U_{22}k^2b^{*2} + U_{33}l^2c^{*2} + 2U_{12}hka^*b^* + 2U_{13}hla^*c^* + 2U_{23}klb^*c^*].$$

Orthorhombic $Bmmb$ (=$Cmcm$), $Z = 4$
X-ray and neutron data from Stehr (1967), $T = 298$ K
Na, O and H at 4(c): $\frac{1}{4}\frac{1}{4}z$, $\frac{3}{4}\frac{1}{4}z + z$, $\frac{3}{4}\frac{3}{4}\bar{z}$, $\frac{1}{4}\frac{3}{4}\frac{1}{4} - z$
$a = 3{\cdot}401$ (1), $b = 3{\cdot}401$ (1), $c = 11{\cdot}382$ (5) Å

	x	y	z	U_{11}	U_{22}	U_{33}
Na	0·25	0·25	−0·087 (1)	0·020 (5)	0·020 (5)	0·015 (6)
O	0·25	0·25	0·117 (1)	0·013 (5)	0·013 (5)	0·017 (6)
H	0·25	0·25	0·197 (1)	0·07 (2)	0·07 (2)	0·016 (6)

$$R = [\Sigma (F_o - F_c)^2/\Sigma F_o^2]^{1/2} = 7\%$$

O–H center-of-mass distance 0·91 (1) Å, probable bond length 0·98 Å

Monoclinic $P2_1/m$, $Z = 2$
Neutron diffraction data (§ 5), $T = 535$ K
Na, O and H at 4(e): $z\frac{1}{4}z$, $\bar{x}\frac{3}{4}\bar{z}$
$a = 3{\cdot}435$ (3), $b = 3{\cdot}445$ (3), $c = 6{\cdot}080$ (5) Å; $\beta = 109{\cdot}9°$

	x	y	z	U_{11}	U_{22}	U_{33}	U_{13}
Na	0·141 (3)	0·25	−0·179 (2)	0·038 (5)	0·030 (6)	0·056 (6)	0·018 (4)
O	0·400 (2)	0·25	0·236 (2)	0·045 (5)	0·030 (6)	0·044 (5)	0·019 (3)
H	0·462 (5)	0·25	0·389 (3)	0·10 (1)	0·11 (1)	0·053 (8)	0·021 (8)

Linear absorption coefficient $\mu = 1{\cdot}38$ cm^{-1}, $R = 6\%$
O–H center-of-mass distance 0·87 (1) Å, probable bond length 0·96 Å

Cubic $Fm3m$, $Z = 4$
X-ray data (§ 4), $T = 578$ K
Na at 000, OH (OD) at $\frac{1}{2}\frac{1}{2}\frac{1}{2}$; $a = 5{\cdot}10$ (2) Å

NaOH	$\langle u^2 \rangle$ (Å^2)	NaOD	$\langle u^2 \rangle$ (Å^2)
Na	0·18 (2)	Na	0·15 (2)
O	0·09 (1)	O	0·08 (1)

2. Experimental

NaOH was supplied by Merck, Darmstadt, with a purity of 99%, the main impurities being H_2O and less than 1% Na_2CO_3. NaOD was prepared by the reaction of Na_2O with D_2O. The crystals were grown by cooling the melt according to the Bridgman and Kyropoulos method in crucibles of gold, silver and also Ni and Al_2O_3. During the cooling process the crystals undergo two phase transitions, and hence their quality was generally poor. Most domains had a volume of only 0·1 to 0·3 cm^3 and a mosaic spread of 1 to 2°. The melt was kept in vacuum at 720 K for several hours, in order to reduce the H_2O content. The preparation of the crystals was done in a glove box in an atmosphere free of H_2O and CO_2. The specific heat was determined by heating or cooling the sample at a roughly constant heat flow, and by numerical differentiation of the temperature curve. The temperature scale was calibrated by the melting points of Pb (600·6 K), Bi (544·2 K) and Sn (505·0 K). The accuracy of the energy scale is 20%. The lattice parameters and the temperature dependence of the monoclinic angle of powder samples were measured on a Philips powder diffractometer using filtered Cu radiation and Bragg–

Brentano focusing geometry. For the determination of the monoclinic order parameter of single crystals, samples with a mosaic spread of 0·1° were selected. The monoclinic angle was obtained from ω scans over the orthorhombic 200 reflection, which splits into two monoclinic $20\bar{1}$ reflections by the formation of twins. In the cubic modification, rotating-crystal photographs were taken using Mo $K\alpha$ radiation.

For the X-ray experiments, the crystals were sealed in thin-walled glass tubes of diameter 2 to 4 mm, or in a small vacuum chamber with Mylar windows. For the neutron diffraction experiments, the sample was enclosed in an Al tube with a wall thickness of 0·15 mm. The monoclinic sample had lengths of 3·5, 8 and 1 mm along **a**, **b** and **c***, respectively, with a mosaic spread of 1°, and it was twinned according to (001). The neutron experiments were performed on the four-circle diffractometer *P*32 at the reactor FR2 in Karlsruhe using a wavelength of 1·035 Å.

3. Lattice parameters and specific heat

The temperature dependence of the lattice constants is shown in Fig. 2. The parameters *a* and *b* of NaOH and NaOD are equal within the error limit of 0·1%. The interlayer distance is smaller in NaOD by 0·3 to 0·6%. At the orthorhombic to monoclinic transition temperature, the interlayer distance $c \sin \beta$ decreases rapidly. The temperature dependence of the monoclinic angle β is discussed in § 7. The orthorhombic unit-cell parameters refer to space group *Bmmb*, which is derived from the standard setting *Cmcm* given in *International Tables for X-ray Crystallography* (1969) by interchanging **b** and **c**. With this choice, the transition to the monoclinic space group $P2_1/m$ is simply described by the change of the angle β.

The specific heat of NaOH is shown in Fig. 3 and a similar curve is obtained for NaOD. The diagram gives the phase transition temperatures and allows one to determine the concentration of H_2O and Na_2CO_3 impurities using the results of Morey & Burlew (1964).

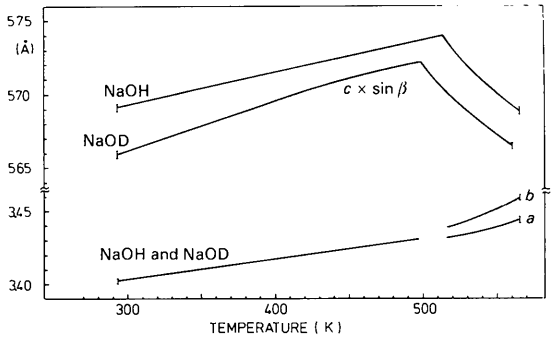

Fig. 2. Temperature dependence of the lattice constants *a*, *b* and the interlayer distance $c \sin \beta$ of NaOH and NaOD.

The four peaks in the diagram correspond to the melting point, the cubic to monoclinic transition, the eutectic point of the system NaOH–Na_2CO_3 and the monoclinic to orthorhombic transition. The melt begins to solidify at 591 K. As a consequence of impurities (mainly 0·4 wt% Na_2CO_3), the melting point is depressed by 1 K. Since Na_2CO_3 is not soluble in solid NaOH, it successively lowers the melting point of the remaining part of the melt, resulting in a low-temperature tail of the peak.

The cubic to monoclinic transition is well defined and this peak has been known from differential thermal analysis curves since the work of von Hevesy (1910). According to Morey & Burlew (1964), up to 2 mol% water are soluble in the cubic phase. Near 559 K the melt contains about 22·6 wt% Na_2CO_3, 77 wt% NaOH and probably 0·4 wt% water, since the freezing temperature is 2 K lower than the temperature of the binary eutectic between NaOH and Na_2CO_3. This would correspond to a total of 0·01 wt% H_2O impurity. The low-temperature tail is due to the insolubility of H_2O in solid NaOH and Na_2CO_3. The peak area corresponds to a total of 0·4 wt% Na_2CO_3 impurity. Since it is not soluble in the crystals, it should not affect the crystal structure determinations. Table 2 gives the phase transition temperatures as determined by different authors.

Table 2. *Transition temperatures of* NaOH *in* K: *orthorhombic to monoclinic transition* T_{o-m}, *monoclinic to cubic transition* T_{m-c}, *melting temperature* T_F *and the eutectic temperature* T_E *of the system* NaOH–Na_2CO_3

T_{o-m}	T_E	T_{m-c}	T_F	References
		572·8	591·6	von Hevesy (1910)
	559	567	593	* Seward (1942). Eutectic 22wt% Na_2CO_3
		566	592	* Douglas & Dever (1954)
		572	595	Reshetnikov & Vilutis (1959)
	559	570	594	Cohen-Adad, Michaud, Said & Rollet (1961). Eutectic 23 wt% Na_2CO_3
	561·1	566	592	* Morey & Burlew (1964). Eutectic 22·7 wt% Na_2CO_3
(572·8)			(591·6)	Stehr (1967). Values are taken from von Hevesy (1910)
513		567	593	Bleif (1971)
518		570	594	Papin & Bouaziz (1973)
514		566	592	Present paper

* Temperature scale has been calibrated by the melting points of metals and the temperatures have been extrapolated to zero Na_2CO_3 content.

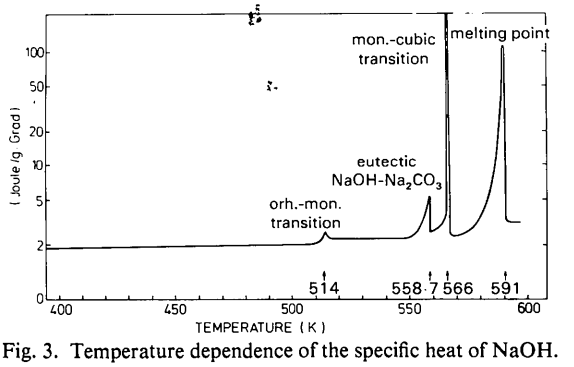

Fig. 3. Temperature dependence of the specific heat of NaOH.

4. Cubic structure

X-ray diffraction results for cubic single crystals are shown in Tables 1 and 3. The intensities were taken from rotating-crystal photographs with rotation axis [100] for NaOH and [111] for NaOD. The predominant features on the photographs are the rapid decrease of the Bragg intensities with increasing diffraction angle, and the diffuse rods passing through the Bragg reflections. This means that there is appreciable thermal motion of the atoms. Since the X-ray scattering of H is negligible, no direct information on its distribution can be obtained. From the symmetry $Fm3m$ one can conclude, however, that the protons cannot be localized at a given lattice site, but have to reorient themselves among symmetrically equivalent sites in order to achieve effective cubic symmetry. The assumption of a reorientational motion of the OH groups is supported by the large heat of transformation observed at the monoclinic to cubic transition.

5. Monoclinic structure

The monoclinic structure was determined from neutron diffraction data at a temperature of 535 K, the distortion of the orthorhombic unit cell being 3·5°. The results of a least-squares structure refinement of 140 non-equivalent reflections are summarized in Table 1.* An absorption correction was applied, taking into account the actual shape of the crystal. The calculations were performed with the XRAY 70 program system (Stewart, Kundell & Baldwin, 1970), with an absorption correction option implemented by G. Kopfmann.

The systematic absence of $0k0$ reflections for odd values of k leads to the space groups $P2_1/m$ or $P2_1$. The structure refinement was done for the space group $P2_1/m$ with all atoms located on the mirror plane at $y = 0{\cdot}25$. A possible deviation from this special position would reduce the space-group symmetry to $P2_1$, and should show up in an anisotropic temperature factor with increased U_{22} components, which is, however, not observed. Fig. 4 shows the monoclinic unit cell with ellipsoids of thermal motion. The H ellipsoid indicates that, for the proton, a riding motion on the oxygen can be assumed. According to Busing & Levy (1964), this results in a probable OH bond length of 0·96 Å, the observed center-of-mass distance being 0·87 Å. Stehr (1967) has determined a projection of the monoclinic structure onto the (010) plane. His results are internally inconsistent, but can be brought into agreement with the present values by referring the atomic coordinates to a monoclinic unit cell with $\beta = 77°$ instead of 110°.

In comparing the monoclinic and orthorhombic modifications, one finds that the phase transition consists of a shear of the orthorhombic structure of 3·5%, with the layers conserving the rock-salt structure with respect to Na and O. The Na—O direction becomes only slightly tilted by 0·6° in the opposite sense to the shear motion. The O—H direction makes an angle of 7° with the normal of the layer, and thus follows the shear motion of the crystal.

The parameters for the orthorhombic structure in Table 1 are taken from Stehr (1967). The primitive unit cell of the orthorhombic modification is obtained from the face-centered cell by the transformation

$$\begin{pmatrix}\mathbf{a}\\ \mathbf{b}\\ \mathbf{c}\end{pmatrix}_{\text{mon}} = \begin{pmatrix}1 & 0 & 0\\ 0 & 1 & 0\\ -0{\cdot}5 & 0 & 0{\cdot}5\end{pmatrix}\begin{pmatrix}\mathbf{a}\\ \mathbf{b}\\ \mathbf{c}\end{pmatrix}_{\text{orth}}$$

and the angle β becomes 106·6°.

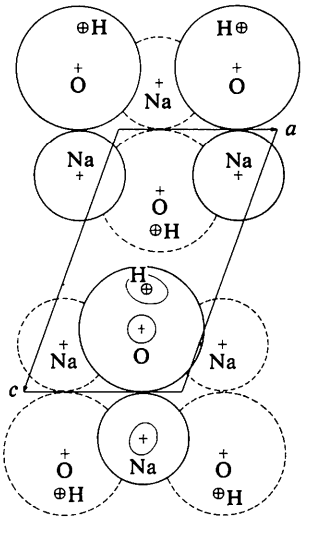

Fig. 4. Monoclinic unit cell of NaOH at T = 535 K with 50% probability ellipsoids of thermal vibration.

* Lists of structure factors for the monoclinic modification have been deposited with the British Library Lending Division as Supplementary Publication No. SUP 36681 (2 pp.). Copies may be obtained through The Executive Secretary, International Union of Crystallography, 5 Abbey Square, Chester CH1 2HU, England.

Table 3. *X-ray structure factors of the cubic modification of* NaOH *and* NaOD

	NaOH		NaOD	
$h\,k\,l$	F_o	F_c	F_o	F_c
2 0 0	38	38	39	39
2 2 0	21	20	22	22
2 2 2	11	11	14	13
4 0 0	6	7	7	8
1 1 1	2	2	3	3·5
1 1 3	0	1	1	0·5

6. Relationship between monoclinic and cubic unit cells

The cubic to monoclinic transition proceeds discontinuously and single crystals usually become polycrystalline. The OH groups become aligned along the monoclinic axis **c***. It was observed on rotating-crystal and Weissenberg photographs that the monoclinic domains tend to maintain a well defined orientation with respect to the original cubic single crystal. The transition was found to proceed in such a way that the monoclinic reciprocal axis **c*** is parallel to the cubic body diagonal [111], the axis **b** is parallel to the cubic face diagonal $[1\bar{1}0]$ and **a** is parallel to $[\bar{1}\bar{1}2]$. Fig. 5 shows two types of monoclinic domains (solid lines) with the unique axis **b** perpendicular to the cubic $(1\bar{1}0)$ plane. To visualize the actual deviations from the orthorhombic structure, the face-centered monoclinic cells are shown (see Fig. 1). A shear of the crystal in the [110] direction by 12° would also lead to the monoclinic structure, but this does not occur in practice. The motions of the atoms associated with this transition could not be determined, but they might be confined to the cubic $(1\bar{1}0)$ plane, since in the direction perpendicular to this plane the crystal already has the appropriate periodicity. The displacements would then occur in the same plane as in the orthorhombic to monoclinic transition. The relative orientation of orthorhombic, monoclinic and cubic unit-cell vectors is summarized in the following matrix equation

$$\begin{pmatrix} \mathbf{a}/a \\ \mathbf{b}/b \\ \mathbf{c}/c \end{pmatrix}_{\text{orth}} = \begin{pmatrix} \mathbf{a}/a \\ \mathbf{b}/b \\ \mathbf{c}^*/c^* \end{pmatrix}_{\text{mon}}$$

$$= \frac{1}{\sqrt{6}} \begin{pmatrix} -1 & -1 & 2 \\ \sqrt{3} & -\sqrt{3} & 0 \\ \sqrt{2} & \sqrt{2} & \sqrt{2} \end{pmatrix} \begin{pmatrix} \mathbf{a}/a \\ \mathbf{b}/b \\ \mathbf{c}/c \end{pmatrix}_{\text{cubic}} .$$

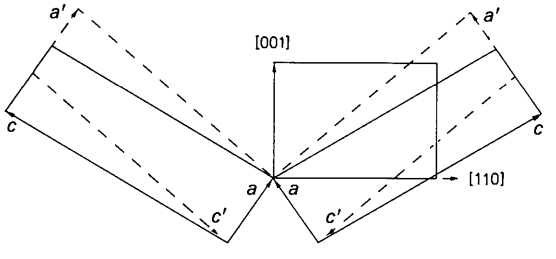

Fig. 5. Relation between cubic and monoclinic unit cells of NaOH and NaOD. Solid lines show the face-centered unit cell of two different monoclinic domains. Dashed lines show monoclinic twins, which develop at the orthorhombic to monoclinic transition.

As the temperature decreases from 566 to 514 K (561 to 500 K for NaOD), the monoclinic angle of the face-centered cell decreases from 95 to 90°. On heating up again, each orthorhombic domain splits into monoclinic twins as shown by the dashed lines in Fig. 5. Weissenberg photographs clearly show that these twins are not formed at the cubic to monoclinic transition. The twins are related by a mirror plane perpendicular to **c***, which is parallel to the former cubic [111] direction. Since there is no mirror plane perpendicular to [111], this also shows that no such twins are formed. This argument also implies that a twinned monoclinic sample does not transform into a cubic single crystal. Furthermore, the transformation relations offer an explanation for the remarkable hysteresis observed in the temperature dependence of the monoclinic order parameter of powder samples and the smearing of the monoclinic to orthorhombic phase transition temperature (see § 7). As a function of temperature, a monoclinic crystallite has to shear by 5° in one direction, and this obviously introduces appreciable stress in the powder sample. If the crystallite consists of twins, the shear motions of the different parts are compensating each other so that the shape of the crystallite can remain unchanged. In going from the orthorhombic to the monoclinic phase, stress is essentially removed by an appropriate twinning.

7. Orthorhombic to monoclinic phase transition

7.1. *General*

The transition from the orthorhombic, low-temperature phase to the monoclinic modification is due to a spontaneous shear of the crystal in the **a** direction (Stehr, 1967). With increasing temperature, the shear angle continuously increases up to 5° near 566 K. A shear of 17° would lead to the cubic *Fm3m* structure for Na and O. It is interesting to compare NaOH with NaF, which has space group *Fm3m* at all temperatures. The F^- ion is of similar size to the OH^-, but it is spherically symmetric. One might expect that OH^- approaches the behavior of F^- if, with increasing temperature, the anisotropy of the OH dipole is effectively reduced by thermal motion. Thus the transition might be looked upon as a first step towards the *Fm3m* structure, caused by a decrease of the OH dipolar character with increasing temperature. The displacement of successive layers in the **a** direction is favored by the stacking sequence in both modifications. It can be seen from Fig. 1 that the OH dipoles of neighboring layers approach each other when the layers are displaced in the **b** direction, whereas they move tangentially to their nearest neighbors when the displacements are in the **a** direction. Without external forces, displacements in the directions $+\mathbf{a}$ and $-\mathbf{a}$ are

equivalent, which results in a twinning of the monoclinic samples.

The order parameter η is the shear of the crystal in the **a** direction and corresponds to the change of the monoclinic angle β. Its temperature dependence has been determined from the diffraction angles of the monoclinic reflections 112 and $11\bar{3}$ and also from ω scans over the 200 reflections of both twins. With single crystals no hysteresis could be detected at a temperature resolution of better than 0·01 K. Probably because of strains or sample dependent inhomogeneities, the reflections are broadened in the temperature range of $T_c \pm 0{\cdot}5$ K, with a reproducible 'coexistence' region of monoclinic and orthorhombic phases of about 0·05 K. Powder samples show a hysteresis of 1·5 K, which is reduced to about 0·1 K after several temperature cycles.

7.2. *Landau expansion*

According to Folk, Iro & Schwabl (1976*a*,*b*) and Cowley (1976), Landau theory should correctly describe structural phase transitions in which the elastic deformation is the primary order parameter. The difference in the free energy of the two modifications is expanded in powers of the order parameter (see, for example, Blinc & Zeks, 1974). A shear in +**a** and −**a** directions is equivalent, so that, in general, odd powers of η are not contained in the expansion. The following expansion was used:

$$g = H\eta + \tfrac{1}{2}A\eta^2 + \tfrac{1}{4}B\eta^4 + \tfrac{1}{6}C\eta^6$$

with

$$A(T) = A_1(T_0 - T)$$

and

$$B(T) = B_0 + B_1(T_0 - T).$$

The low-temperature modification of NaOH has the higher symmetry, so that the temperature dependence of the order parameter is reversed compared to most other structural phase transitions. T_0 is the stability limit of the high-symmetry phase. The actual transition temperature, T_c, differs from T_0 if the transition is discontinuous.

In addition to the usual expansion, a temperature dependence of the coefficient B of the fourth-order term had to be taken into account. The sixth-order term is necessary because the transition is discontinuous. Its coefficient C is assumed to be temperature independent. In order to describe the smearing of the transition temperature of the powder samples, an external field parameter H is introduced in the Landau free-energy expansion, which directly couples to the order parameter. The temperature dependence of η is determined by the condition

$$\frac{\partial g}{\partial \eta} = 0 \quad \text{and} \quad \frac{\partial^2 g}{\partial \eta^2} = \chi^{-1} > 0.$$

The inverse susceptibility, χ^{-1}, corresponds to the elastic shear modulus, c_{55}. The least-squares fit of the experimental data to the relation

$$H\eta^{-1} + A_1(T_0 - T) + [B_0 + B_1(T_0 - T)]\eta^2 + C\eta^4 = 0$$

was done by fitting the temperature, T, as a function of the order parameter, η. The influence of the experimental errors and of the non-uniform separation s of the data points was taken into account by the weights

$$w = s \Big/ \left[\Delta T^2 + \left(\frac{\partial T}{\partial \eta} \Delta \eta \right)^2 \right]$$

with the experimental errors $\Delta T = 0{\cdot}1$ K and $\Delta\eta = 0{\cdot}1°$.

Three different data sets were simultaneously fitted to the above expression with individual external field parameters H. The results are plotted in Figs. 6 and 7.

The following parameters were obtained from the fit, with the estimated standard deviations given in units of the last digit (the constant A_1 is set equal to 1):

Transition temperature, measured with thermocouple calibrated with the melting point of Sn (505·0 K): $T_c = 514{\cdot}7$ (2) K

Stability limit of the orthorhombic phase: $T_0 = T_c + 0{\cdot}6$ (1) K

Strain-field parameter for powder samples
cooled down from the cubic phase: $H = -0{\cdot}87$ (4)
for annealed powder samples: $H = -0{\cdot}22$ (3)
for single crystals: $H = -0{\cdot}025$ (3)

Expansion coefficients: $B_0 = -1{\cdot}3$ (1), $B_1 = 0{\cdot}18$ (1), $C = 0{\cdot}53$ (2).

The transition turns out to be discontinuous with a jump of the shear angle of about 0·9°. In Fig. 6 this is expressed by the negative slope of the calculated order parameter. The phase transition temperature is 0·6 K below the stability limit. The external field parameter for the single-crystal data is small and is observed experimentally as a reversible broadening of the reflections prior to the splitting. When cooled down from the cubic phase, the powder samples show a remarkable hysteresis of 1 K, which disappears once

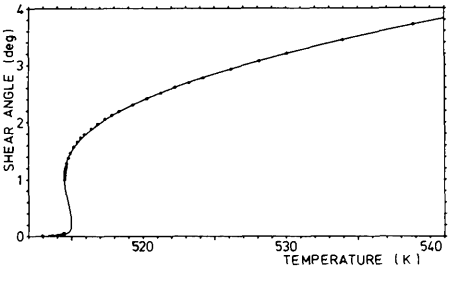

Fig. 6. Order parameter of the orthorhombic to monoclinic transition of NaOH single crystals.

the sample has been in the orthorhombic modification. As mentioned in § 6, this is explained by a mutual hindrance of the crystallites during their shear motion, which is greatly relieved as soon as monoclinic twins can develop.

8. Concluding remarks

The present paper gives a summary of the structural phase transitions of NaOH and NaOD. In going from orthorhombic to cubic symmetry, the OH (OD) group approaches the behavior of a spherically symmetric ion. As a consequence of this tendency, the layers approach one another in the monoclinic phase and finally collapse in the cubic transition. There is a strong diffuse X-ray scattering with maximum intensity at the orthorhombic to monoclinic transition temperature, which is due to the softening of an acoustic shear mode. A preliminary analysis has been given by Bleif, Dachs & Knorr (1971). The study of the cubic modification will be completed in a subsequent paper, using neutron scattering results which will also yield the probability density distribution of the hydrogen.

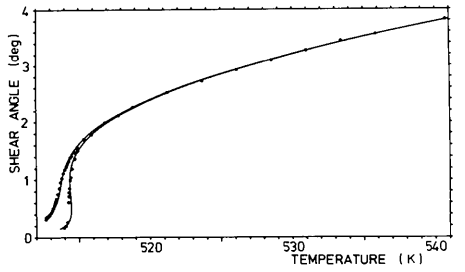

Fig. 7. Order parameter of the orthorhombic to monoclinic transition of NaOH powder samples.

The authors would like to thank Professor F. Schwabl for stimulating discussions.

References

BLEIF, H.-J. (1971). Diplomarbeit. Univ. Tübingen.

BLEIF, H.-J., DACHS, H. & KNORR, K. (1971). *Solid State Commun.* **9**, 1893–1897.

BLINC, R. & ZEKS, B. (1974). *Soft Modes in Ferroelectrics and Antiferroelectrics*. Amsterdam: North-Holland.

BUSING, W. R. & LEVY, H. A. (1964). *Acta Cryst.* **17**, 142–146.

COHEN-ADAD, R., MICHAUD, M., SAID, J. & ROLLET, A.-P. (1961). *Bull. Soc. Chim. Fr.* pp. 356–359.

COWLEY, R. A. (1976). *Phys. Rev. B*, **13**, 4877–4885.

DOUGLAS, TH. B. & DEVER, J. L. (1954). *J. Res. Natl Bur. Stand.* **53**, 81–90.

ERNST, TH. (1946). *Nachr. Ges. Wiss. Göttingen, Math.-Phys. Kl.* pp. 76–78.

FOLK, R., IRO, H. & SCHWABL, F. (1976*a*). *Phys. Lett.* **57A**,112–114.

FOLK, R., IRO, H. & SCHWABL, F. (1976*b*). *Z. Phys.* **B25**, 69–81.

HEVESY, G. VON (1910). *Z. Phys. Chem.* **73**, 672–684.

International Tables for X-ray Crystallography (1969). Vol. 1. Birmingham: Kynoch Press.

MOREY, G. W. & BURLEW, J. S. (1964). *J. Phys. Chem.* **68**, 1706–1712.

PAPIN, G. & BOUAZIZ, R. (1973). *C. R. Acad. Sci. Ser. C*, pp. 771–774.

RESHETNIKOV, N. A. & VILUTIS, N. I. (1959). *Russ. J. Inorg. Chem.* **4**, 49–53.

SEWARD, R. P. (1942). *J. Am. Chem. Soc.* **64**, 1053–1057.

STEHR, H. (1967). *Z. Kristallogr.* **125**, 332–359.

STEWART, J. M., KUNDELL, F. A. & BALDWIN, J. C. (1970). XRAY 70. Modified version of XRAY 67 of the Univ. of Maryland with an absorption correction program by G. Kopfmann, MPI München.

WEST, C. D. (1935). *J. Phys. Chem.* **39**, 493–507.